Journal of Materials Science: Materials in Electronics
https://doi.org/10.1007/s10854-018-8694-z

# Optimal conditions for fabricating CIGS nanoparticles by solvothermal method

**E. Ghanbari[1] · M. Zahedifar[1,2] · O. Amiri[1]**

Received: 1 November 2017 / Accepted: 28 January 2018


**Abstract**
CIGS nanoparticles (NPs) were synthesized by solvothermal method. The effects of using argon and nitrogen as autoclave atmosphere and also metallic indium ($In_{met}$) and $InCl_3$ as indium precursors at different temperature profiles on crystalline phase of the fabricated CIGS NPs were investigated. Results show that producing single phase CIGS in $N_2$ atmosphere is not possible. In Ar atmosphere, $CuIn_{0.5}Ga_{0.5}Se_2$ pure phase was formed only by using $InCl_3$ as indium precursor. In addition to CIGS, $CuGaSe_2$ can also be observed, but CIS phase is not formed by using this approach. The particle size in the range of 20–45 nm was detected by XRD and SEM images. UV–visible absorption spectrum showed a broad peak in UV–visible range. Also reported is the unusual behavior of the produced NPs in different atmospheres.

## 1 Introduction

$CuIn_xGa_{1-x}Se_2$ compound as a semiconductor has many benefits compared to other materials (e.g. CdTe, GaAs …) as absorber layer in thin film solar cells. CIGS with advantages such as variable band gap from 1.04 to 1.68 eV [1], minimized material consumption and high absorption efficiency, low cost substrate (e.g. soda-lime glass) and flexible substrate (e.g. metals foil) and good stability, is a very promising material for fabricating solar cells with high energy conversion efficiency [2–7].

Electrodeposition and coating CIGS ink are the most important non-vacuum methods employed to make CIGS thin film [8–11]. Deposition of CIGS Nps is one of the non-vacuum approaches to produce CIGS layer [12, 13]. In this approach, first CIGS Nps are synthesized and then coated as a layer by several methods such as spray or spin coating [14, 15]. For synthesis of CIGS nanoparticle, solvothermal method was usually adopted because of CIGS phase, stoichiometry of elements and particles size are easy to control by this method [16]. Sin-il Gu et al. [17] changed synthesis temperature from 190 to 250 °C at 8–40 h to synthesize CIGS single phase but in all samples, CIS and CGS phases were also present along with CIGS phase. Chun et al. [18] used one step annealing at 140–280 °C for 36 h to fabricate CIGS Nps. They found that production of spherical CIGS Nps in ethylenediamine by solvothermal method is possible. Mousavi et al. [19] studied the effects of using $NH_4Cl$, $NH_4I$ and $NH_4Br$ on synthesis time and succeed to reduce synthesis time to 2 h. Sing-Il et al. [20] investigated using gallium metallic as precursor on synthesized CIGS and found that production of CIGS pure phase by gallium metal is not possible. All the experiments to construct CIGS Nps by solvothermal are usually carried out in argon or nitrogen atmosphere. Our experiences showed that besides optimizing different conditions for fabricating high quality CIGS NPs, stainless steel autoclave atmosphere also plays important role which should be taken into consideration hereafter. So, in this work, the effects of using argon and nitrogen atmospheres on fabrication of CIGS Nps were studied. Furthermore it was studied that how the metallic indium and $InCl_3$ as precursors and changing synthesis temperature can affect the CIGS phase. By changing these parameters we succeed to achieve CIGS single phase with different ratios of indium to gallium. This ratio which controls the band gap of CIGS, is one of the most important parameters in CIGS solar cells.

✉ M. Zahedifar
zhdfr@kahanu.ac.ir

[1] Institute of Nanoscience and Nanotechnology, University of Kashan, Kashan 87317, Iran

[2] Physics Department, University of Kashan, Kashan 87317, Iran

Published online: 30 January 2018

## 2 Experimental

Considering our previous work [21], solvothermal method was used to synthesize CIGS Nps. The mixtures, including 0.032 g (0.50 mmol) copper powders, 0.078 g (1 mmol) selenium powders, 0.028 g (0.025 mmol) metallic indium (mesh 0.1 mm) or 0.056 g (0.025 mmol) indium chloride (InCl3) and 0.044 g (0.025 mmol) gallium chloride (InCl3) were solved in 50 ml of ethylenediamine ($C_2H_8N_2$) as solvent, all from Merck Company. The mixture was stirred at atmosphere for 1 h at room temperature and then was put in sealed stainless steel autoclave. The effect of filling the autoclave atmosphere with Ar or $N_2$ on the ratio of In to Ga was also considered. A two-step heating process was used to produce CIGS Nps. At first step, the mixtures were heated at temperatures between 155 and 185 °C for 12 h. In the next step, the temperature was kept at 230 °C for 24 h. The products were washed 4 times with deionized water and finally dried at 100 °C for 24 h at atmosphere. Structure of Nps were analyzed using X-ray diffractometer Philips X'Pert Bruker D8 Advance with $CuK_\alpha$ radiation ($\lambda = 1.54A^o$) under the condition of 40KV and 30 mA at a step size of $2\theta = 0.02°$. Size and morphology of particles were observed by using field emission scanning electron microscope (MIRA3TESCAN-XMU). The FESEM equipped with an EDS detector was employed for analyzing the element concentration. UV–visible spectrometer was used to study the absorption of CIGS NPs and to obtain the band gap.

## 3 XRD results

In our experiments, the effects of using $N_2$ and Ar as inert atmosphere and also using metallic indium and indium chloride as In precursor on the phase of the produced Nps were studied. For doing this, 16 samples were prepared. 3 samples were synthesized by $In_{met}$ in Ar atmosphere and 3 samples were synthesized by In in $N_2$ atmosphere. Remaining 10 samples were synthesized by $InCl_3$ in Ar and $N_2$ atmospheres. Each sample was first heated in a specific temperature between 155 and 185 °C for 12 h, then annealing was continued for 24 h at 230 °C. A list of synthesis conditions including precursors, autoclave atmosphere and heating profiles is summarized in Table 1.

Shown in Fig. 1 are the XRD patterns of samples 1–3. These samples were synthesized by $In_{met}$ in $N_2$ atmosphere. According to the standard values of reported data (JCPDS Card No. 00-035-1100), XRD pattern of $CuGaSe_2$ (CGS) has five major diffraction peaks from: (112), (204), (312), (400) and (322) crystalline planes at $2\theta = 27.7°$, 46.1°, 54.2°, 66.6° and 74.2°, respectively. Crystalline growth of CIGS by X = 7/3 (X = ratio of In to Ga) have same Miller indices as CGS at $2\theta = 26.8°$, 44.6°, 52.9°, 64.9° and 71.7°, respectively (JCPDS Card No. 00-035-1102). The XRD results show co-existence of CIGS and CGS phases. For these samples changing the first step temperature from 175 to 185 °C does not have any effect on crystalline phase. Co-formation of CIGS and CGS is attributed to the structure of metallic Indium and $GaCl_3$. Indium with metallic binding has low solubility in

**Table 1** Precursors, heating profile and autoclave atmosphere of synthesized samples

| Samples | Precursors | First step annealing ( °C) | Final step annealing ( °C) | Autoclave atmosphere |
|---|---|---|---|---|
| 1 | Cu, In metallic, $Gacl_3$, Se | 185 | 230 | Nitrogen |
| 2 | Cu, In metallic, $Gacl_3$, Se | 180 | 230 | Nitrogen |
| 3 | Cu, In metallic, $Gacl_3$, Se | 175 | 230 | Nitrogen |
| 4 | Cu, $InCl_3$, $Gacl_3$, Se | 185 | 230 | Nitrogen |
| 5 | Cu, $InCl_3$, $Gacl_3$, Se | 180 | 230 | Nitrogen |
| 6 | Cu, $InCl_3$, $Gacl_3$, Se | 175 | 230 | Nitrogen |
| 7 | Cu, In metallic, $Gacl_3$, Se | 185 | 230 | Argon |
| 8 | Cu, In metallic, $Gacl_3$, Se | 180 | 230 | Argon |
| 9 | Cu, In metallic, $Gacl_3$, Se | 175 | 230 | Argon |
| 10 | Cu, $InCl_3$, $Gacl_3$, Se | 185 | 230 | Argon |
| 11 | Cu, $InCl_3$, $Gacl_3$, Se | 180 | 230 | Argon |
| 12 | Cu, $InCl_3$, $Gacl_3$, Se | 175 | 230 | Argon |
| 13 | Cu, $InCl_3$, $Gacl_3$, Se | 170 | 230 | Argon |
| 14 | Cu, $InCl_3$, $Gacl_3$, Se | 165 | 230 | Argon |
| 15 | Cu, $InCl_3$, $Gacl_3$, Se | 160 | 230 | Argon |
| 16 | Cu, $InCl_3$, $Gacl_3$, Se | 155 | 230 | Argon |

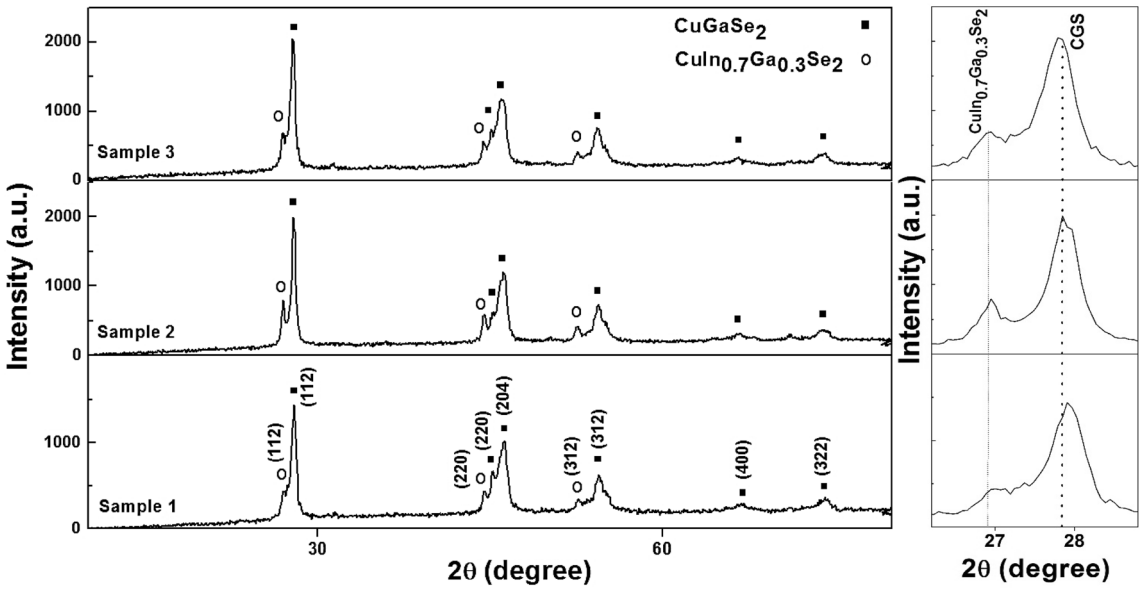


**Fig. 1** XRD patterns of CIGS Nps synthesized by $In_{met}$ at 185 °C (sample 1), 180 °C (sample2), 175 °C (sample3) in Nitrogen atmosphere

ethylenediamine, while $GaCl_3$ with ionic bonds has high solubility in this solvent, so gallium releases more than indium and participates in the reaction process. In the first step heating, to produce CIGS Nps, Se and Cu dissolve in ethylenediamine to form $Se^{2-}$ and $[Cu(en)_2]^+$, respectively according to Eq. (1). Ga and In react with $Se^{2-}$ to procedure unstable $Ga_2Se_3$ and $In_2Se_3$ (Eqs. 2, 4). In the next step annealing, with increasing temperature to 230 °C, others $Se^{2-}$ ions react with $Ga_2Se_3$ and $In_2Se_3$ to form $GaSe_2$ and $InSe_2$ (Eqs. 3, 5). At the end, $CuIn_{0.7}Ga_{0.3}Se_2$ and $CuGaSe_2$ were formed [22, 23]. When Ga releases more than In, some of Ga ions react to form CIGS (Eq. 6) and the remaining Ga react to form CGS (Eq. 7), so two phases of CGS and CIGS are synthesized together.

$$Cu^+ + 2(en) \Rightarrow [Cu(en)_2]^+ \quad (1)$$

$$2GaCl_3 + 3Se^{2-} \Rightarrow Ga_2Se_3 + 6Cl^- \quad (2)$$

$$Ga_2Se_3 + Se^{2-} \Rightarrow 2(GaSe_2)^- \quad (3)$$

$$2InCl_3 + 3Se^{2-} \Rightarrow In_2Se_3 + 6Cl^- \quad (4)$$

$$In_2Se_3 + Se^{2-} \Rightarrow 2(InSe_2)^- \quad (5)$$

$$10[Cu(en)_2]^+ + 7(InSe_2)^- + 3(GaSe_2)^- \Rightarrow 10CuIn_{0.7}Ga_{0.3}Se_2 + 20(en) \quad (6)$$

$$[Cu(en)_2]^+ + (GaSe_2)^- \Rightarrow CuGaSe_2 + 2(en) \quad (7)$$

XRD patterns of samples 1–3 show that the amount of In in reaction process is less than Ga, hence In remains in the metallic state. As mentioned, gallium chloride has more solubility in solvent compared to the metallic indium, so for balancing between In and Ga, $InCl_3$ was used instead of metallic indium because $InCl_3$ has ionic bonds with high solubility in ethylenediamine. By using $InCl_3$ instead of $In_{met}$, CGS and CIGS phases with X = 7/3 were formed together again, however sharp XRD peaks of CIGS confirms that crystallinity of CIGS is better than CGS (Fig. 2). In addition, the amount of In to Ga in these samples is more than those of samples 1–3 (Table 2), therefor it is expected that the amount of CIGS in these samples to be more than CGS compare to samples 1–3.

Results revealed that single phase CIGS cannot be produced in nitrogen atmosphere, thus in the next step, argon was used instead of nitrogen. XRD patterns of samples 7–9 are shown in Fig. 3. These samples were synthesized by $In_{met}$ in Ar atmosphere. Our findigs confirm that using $In_{met}$ in different heating profiles in both Ar and $N_2$ atmospheres causes co-formation of CGS and CIGS, however the samples7–9 produced in Ar atmosphere are different from samples 1–3. In samples 7–9, X = 1 while this ratio is 7/3 for samples 1–3. By using $N_2$ as atmosphere, indium reacts with $N_2$ to form $In^{+3}$–$N_2$ complex according to Eqs. 8, 9. But when Ar is employed instead of $N_2$, ethylenediamine is banded to $In^{3+}$ and form In-en complex (Eqs. 10, 11).

$$In^{3+} + N_2 \Rightarrow In^{3+}{-}N_2(complex) \quad (8)$$

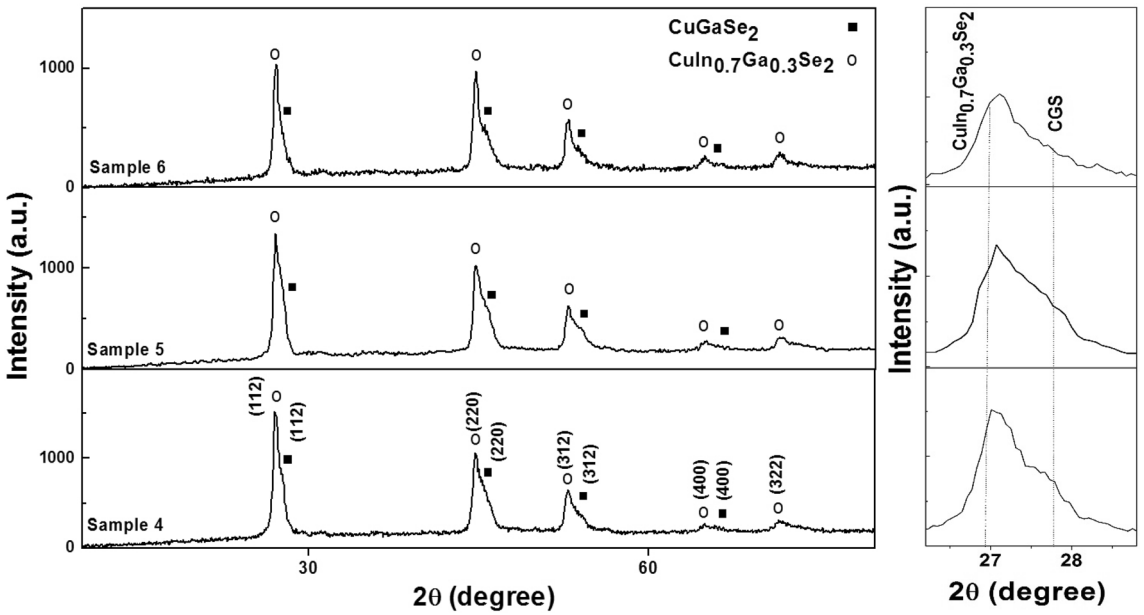


**Fig. 2** XRD patterns of CIGS Nps synthesized by $InCl_3$ at 185 °C (sample 4), 180 °C (sample5), 175 °C (sample6) in Nitrogen atmosphere

**Table 2** Concentration of Cu, In, Ga and Se along with the ratios of Ga/(Ga + In), cu/(In + Ga), se/Metall, band gap and particles size of the samples 2,5,8, 10–16

| Samples | Cu | In | Ga | Se | Ga/(Ga+In) | Cu/(In+Ga) | Se/Metall | Band gap (eV) | Particle size (nm) |
|---|---|---|---|---|---|---|---|---|---|
| 2 | 43.17 | 12.07 | 7.90 | 36.86 | 0.39 | 2.10 | 0.58 | 1.14 | 40.37 |
| 5 | 33.41 | 15.72 | 8.65 | 42.22 | 0.35 | 1.37 | 0.81 | 1.12 | 43.61 |
| 8 | 38.05 | 5.63 | 16.42 | 39.90 | 0.74 | 1.71 | 0.66 | 1.53 | 25.20 |
| 10 | 30.72 | 5.62 | 18.58 | 45.08 | 0.76 | 1.25 | 0.82 | 1.78 | 23.50 |
| 11 | 30.92 | 14.95 | 11.39 | 42.74 | 0.43 | 1.17 | 0.74 | 1.55 | 27.68 |
| 12 | 23.05 | 16.85 | 11.75 | 48.35 | 0.41 | 0.80 | 0.93 | 1.39 | 20.62 |
| 13 | 30.05 | 15.10 | 9.83 | 45.02 | 0.40 | 1.23 | 0.81 | 1.36 | 24.71 |
| 14 | 31.16 | 16.26 | 9.05 | 43.53 | 0.35 | 1.23 | 0.77 | 1.27 | 30.72 |
| 15 | 40.07 | 16.35 | 7.09 | 36.49 | 0.30 | 1.70 | 0.57 | 1.25 | 24.46 |
| 16 | 40.96 | 19.77 | 7.07 | 32.20 | 0.26 | 1.52 | 0.47 | 1.22 | 29.30 |

$$In^{3+} - N_2(complex) + 3Se^{2-} \Rightarrow In_2Se_3 + N_2 \quad (9)$$

$$In^{3+} + 3en \Rightarrow \left[In(en)_3\right]^{3+} \quad (10)$$

$$2\left[In(en)_3\right]^{3+} + 3Se^{2+} \Rightarrow In_2Se_3 + 6en \quad (11)$$

$In^{+3}$–$N_2$ is a weak complex compared to $[In(en)_3]$, accordingly in samples 1–3 more In releases and participate in reaction process to result increasing In to Ga ratio compared to samples 7–9.

In samples 10–12 by using $InCl_3$ in Ar atmosphere, single phase CIGS by different values of X were obtained (Fig. 4). As shown in Fig. 4, $CuIn_{0.5}G_{0.5}Se_2$ have XRD pattern with peaks diffracted from (112), (220), (312), (400) and (332) planes located at 2θ = 27.1°, 46.1°, 54.2°, 66.6° and 74.2° (JCPDS Card No. 00-040-1488). Sample10, synthesized at 185 °C, is a single phase CGS. By decreasing temperature to 180 °C (sample 11) two phases of CIGS with X = 1 and CGS were obtained. More decrease in temperature to 175 °C causes vanishing of CGS phase, while the single phase $CuIn_{0.5}G_{0.5}Se_2$ remains. XRD results of samples 10–12 confirmed that at 185 °C, CGS phase is synthesized and by decreasing temperature to 175 °C the amount of In increases (Table 2), so it is possible to produce CIS in lower temperatures. Thus we reduced temperature to 155 °C in samples 13–16 to investigate the formation of CIS.

In sample 13 by decreasing temperature to 170 °C, CIS with CIGS phases were synthesized together (Fig. 5). In this sample X = 7/3 for CIGS that shows the increased quantity

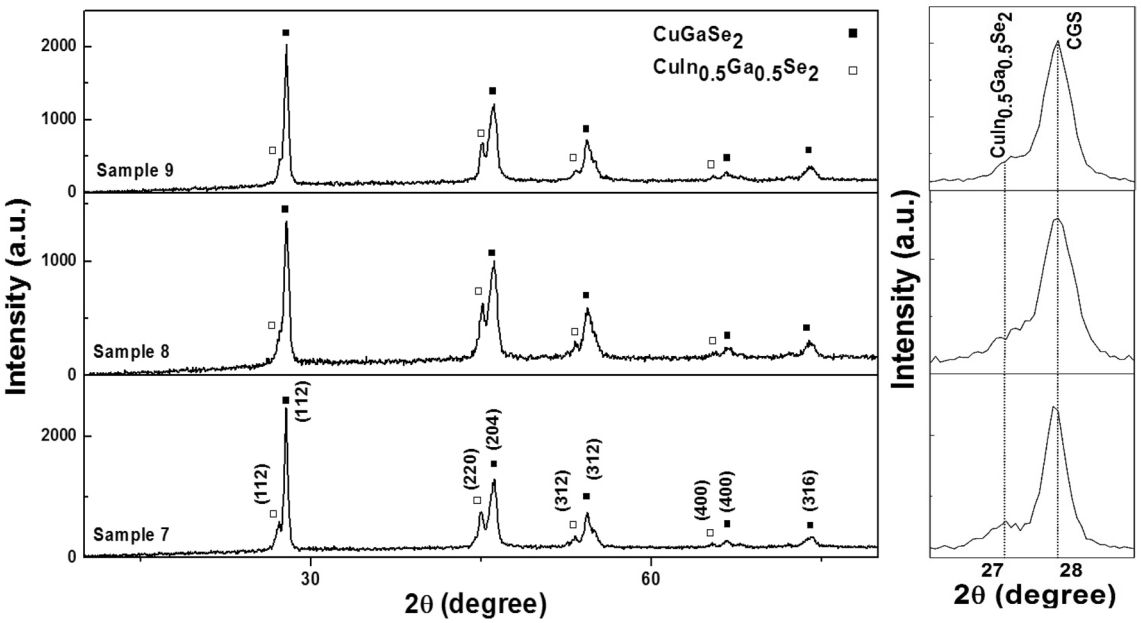


**Fig. 3** XRD patterns of CIGS Nps synthesized by $In_{met}$ at 175 °C (sample 7), 180 °C (sample8), 185 °C (sample9) in Argon atmosphere

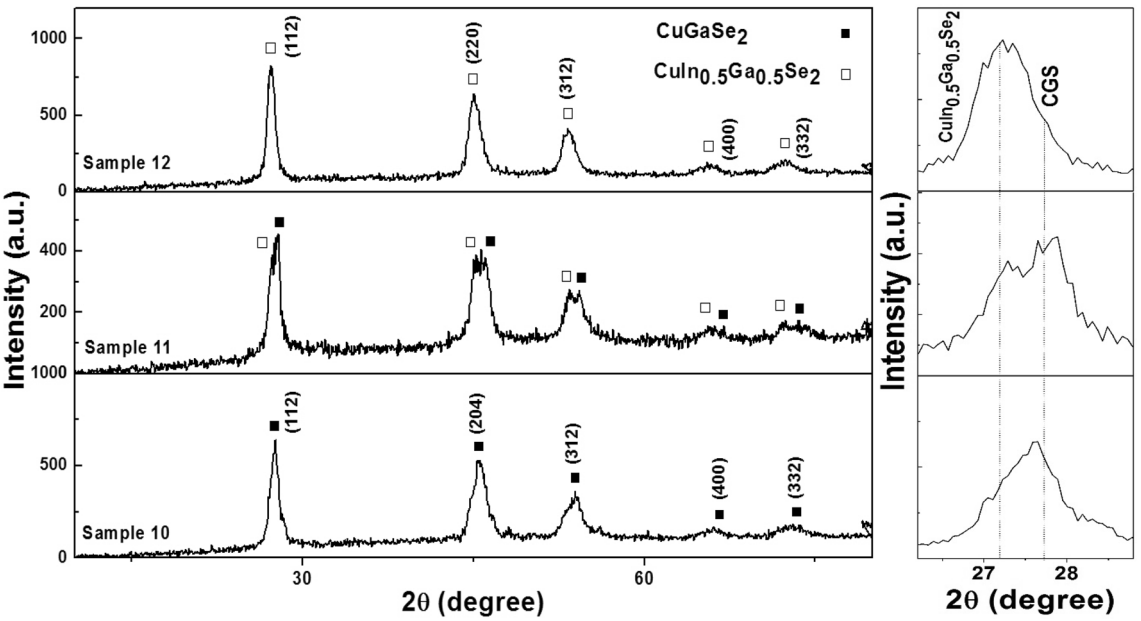


**Fig. 4** XRD patterns of CIGS Nps synthesized by $InCl_3$ at 185 °C (sample 10), 180 °C (sample11), 175 °C (sample12) in Argon atmosphere

of In. As mentioned, in Ar atmosphere $In(en)_3$ is formed. At 155 °C, this complex doesn't form and indium remains in the form of $In^{3+}$.These ions are added to react and form CIGS, so the amount of X increases. By increasing temperature to 185 °C, this complex is formed and its chemical bonds become stronger which results in decreasing $In^{3+}$ in solvent, so by increasing temperature from 155 to 185 °C, firstly CIS and CIGS were formed, indicating that the value of indium in the mixture is high, while at 185 °C, the amount of indium in reaction reaches zero and only CGS is formed. Formation of CIS phase with cubic structure is a remarkable event in this sample. Cubic CIS have five major diffraction peaks from (111), (220), (311), (400) and (331) planes located at $2\theta = 27.6°$, 45.8°, 54.5°, 67.0° and 74.0° (JCPDS Card No. 00-023-0208). It is common that CIGS, CGS and CIS are formed with tetragonal structure like samples 1–12, but in

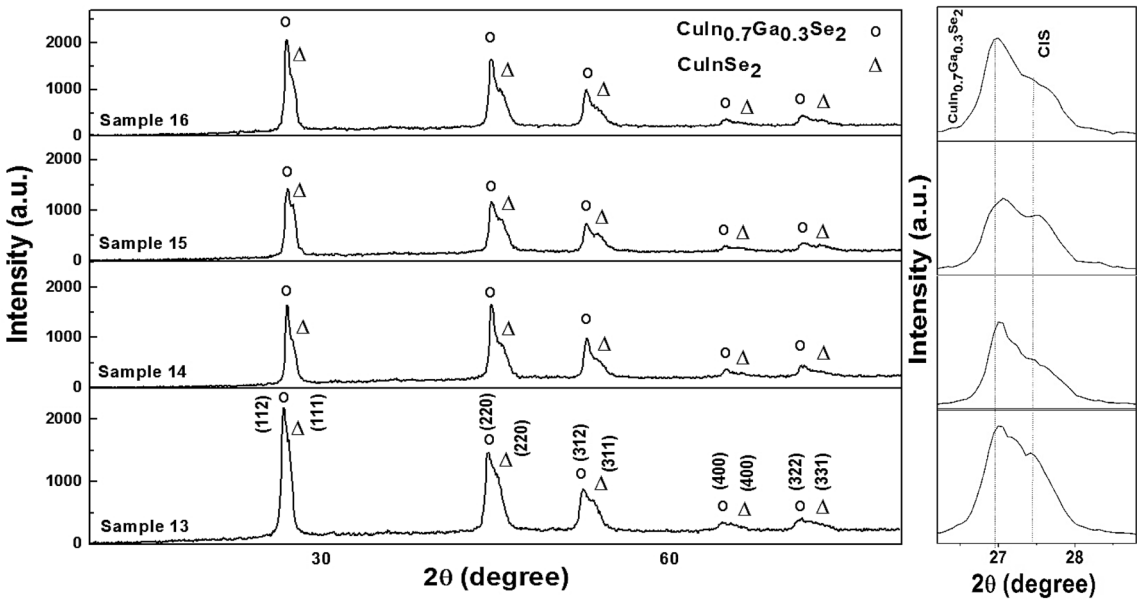


**Fig. 5** XRD patterns of CIGS Nps synthesized by InCl3 at 170 °C (sample 13), 165 °C (sample14), 160 °C (sample15), 155 °C (sample16) in Argon atmosphere

this sample tetragonal CIGS was synthesized with cubic CIS. In samples 14–16, temperature were decreased by 5 °C for each sample but in all samples CIGS were synthesized together with CIS without any change in X or phase, indicating that it isn't possible to fabricate CIS by this approach.

## 4 EDX results

Chemical composition of samples was determined by EDS and inserted in Table 2. Amongst samples 1–3, 4–6 and 7–9, only element concentrations for samples 2, 5, 8 (for these samples first step annealing was 180 °C) were inserted in table since the phases of these samples remained unchanged during different heating processes. These outcomes confirm that the ratio of In to Ga is higher for the samples produced using $InCl_3$ (samples 5 and 10–16) compared to samples synthesized by $In_{met}$ (samples 2 and 8). Furthermore Cu/In/Ga/Se ratio for all samples agree well with XRD patterns.

3 ratios including: Ga/Ga + In (GGI), Cu/Ga + In (CGI) and Se/Cu + Ga + In (Se/Metal) are very important to construct highly efficient CIGS thin film solar cells. These ratios were calculated for all samples and are listed in Table 2. In CIGS layer if CGI > 1 the layer is Cu-rich and if CGI < 1 the layer is Cu-poor. The Cu-rich layer is large grain p-type structure but it causes shunts in CIGS solar cell whereas Cu-poor layer as n-type layer, small grain and smooth surface doesn`t generate shunts in devices [24–26]. Among the studied samples, sample 12 can be used for fabricating Cu-poor layer and other samples are Cu-rich. Se/Metal ratio affects the resistivity of CIGS solar cell and CIGS p-type or n-type are influenced by this ratio. Se-rich (Se/Metal > 1) layers are p-type and Cu-poor(Se/Metal < 1) layers are n-type [27, 28].

The band gap of CIGS layer can be adjusted by tuning the GGI ratio. By changing GGI from 0 to 1, CIGS band gap changes from 1.04 to 1.68 eV. The best amount for GGI is about 0.3–0.4 [29]. By this amount, maximum efficiency of CIGS solar cell can be achieved. In all samples, except 8 and 10, GGI has good rate for fabrication a highly efficient CIGS solar cell.

## 5 Optical properties

Optical properties of samples were studied by optical absorption spectroscopy. In Fig. 6 because of large number of samples, only absorption spectrums of samples 10 and 12 are shown. For these samples single phase CGS and CIGS were synthesized respectively. All samples show absorption peak in UV–visible range. Tauc relation, $(\alpha h\nu)^2 = A(E - E_g)$, was used to calculate band gap of the samples where α is the absorption coefficient, A is a constant, $E_g$ is band gap and n is a constant which takes the value 0.5 for indirect band gap and 2 for direct band gap CIGS [30]. The band gap was estimated from the intercept of the linear portion of $(\alpha h\nu)^2$ vs. hν plots on the hν axis. The band gap was estimated about 1.78 and 1.39 eV for samples 10 and 12 respectively (Fig. 7). The band gap of the other samples are listed in Table 2. For samples 10–16 as mentioned above, by decreasing temperature from 185 °C to 155 °C, the amount of Indium was

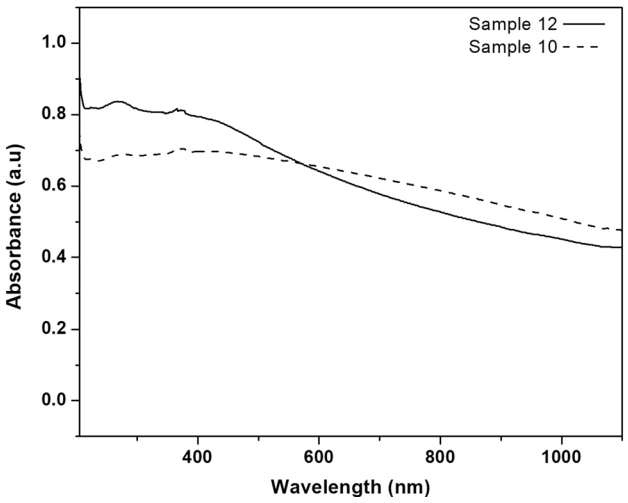


**Fig. 6** Absorption spectrums of samples 10 (CGS Nps) and 12 (CIGS Nps)

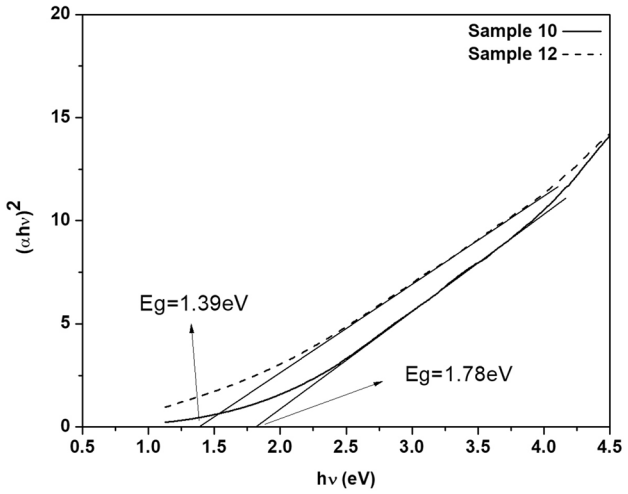


**Fig. 7** Plots of $(\alpha h\nu)^2$ against $h\nu$ for samples 10 and 12

increased, resulting decrease in the band gap from 1.78 to 1.25 eV. The band gap of CGS NPs produced as samples 10 is about 1.78 eV which is close to the reported value for band gap of CGS. By decreasing temperature, this value decreased to 1.22 eV that is closed to CIS band gap. This variation confirms that by increasing In, band gap of CIGS Nps decreases.

Fabrication of CIGS with different band gap is very important because in CIGS solar cell panels different GGI ratios are used. Usually, the band gap in high-efficiency CIGS solar cells is about 1.1–1.2 eV corresponding to a GGI ration of around 0.3 but many researchers and factories use CIGS solar modules with the band gap between 1.1 and 1.7 eV for high -efficiency cells [31]. The reason for this is attributed to the area where CIGS solar cells are supposed to be used because the solar spectrum varies from place to place so for achieving maximum conversion efficiency, CIGS with optimum band gap should be used [32, 33]. For best band gap it is necessary to control ratio of GGI that achieved in our nanoparticles. Accordingly samples 2, 5 and 12–16 can be used as low band gap CIGS layers and samples 8, 10, 11 can be used for high band gap solar cells.

## 6 FESEM images

Figure 8 shows FESEM images of the synthesized CIGS Nps. For samples 2 and 5 synthesized in $N_2$ atmosphere, rod-shape and irregular shape Nps were grown together. But only rod lumps of small spherical Nps are observed in samples 8, an indication of agglomeration of NPs in this sample. By increasing first step annealing temperature to 180 °C in sample 11 and 185 °C in sample 10, the Nps firstly agglomerate to plate-like shape in sample 11 and then grow to large plates in sample 10. For these samples in addition to the plate- like Nps, irregular shape particles are also presented. Sample 12 is the only one including spherical particles with average size of 23 nm without any rod-shape Nps. Plate-like shape along with agglomerated Nps in irregular shapes are also exist in samples 13–16.

As stated above, different degrees of agglomeration of Nps can be observed in all of the synthesized samples. It should be mentioned that agglomeration of CIGS Nps is common in solvothermal method. There are 2 reasons for agglomeration of particles: the first is that ethylenediamine solvent cannot act as a surfactant and prevent agglomeration of Nps. Secondly, according to the Ostwald ripening mechanism, after formation of primary particles, high synthesis temperature and surface energy of particles lead to agglomeration [34, 35].

The average size of Nps were calculated using Scherrer's formula and are observed in Table 2. All samples show average size in the range of 20 to 45 nm which is in accordance with particles size in FESEM images. The average size for samples synthesized in $N_2$ atmosphere is larger than those synthesized in Ar. Solvothermal method is an isovolumetric process. The energy transfer by heating in constant volume is given by $Q = nC_v(T_2 - T_1)$ where n is the amount of gas in mol, $C_v$ is the specific heat capacity at constant volume, $T_1$ is the initial temperature and $T_2$, the final temperature. $C_v$ for diatomic gas like $N_2$ is more than monatomic gas like Ar, so Q in $N_2$ atmosphere is more than that of Ar atmosphere, leading to an increased surface energy, which in turn causes the primary particles to grow and produce larger particles.

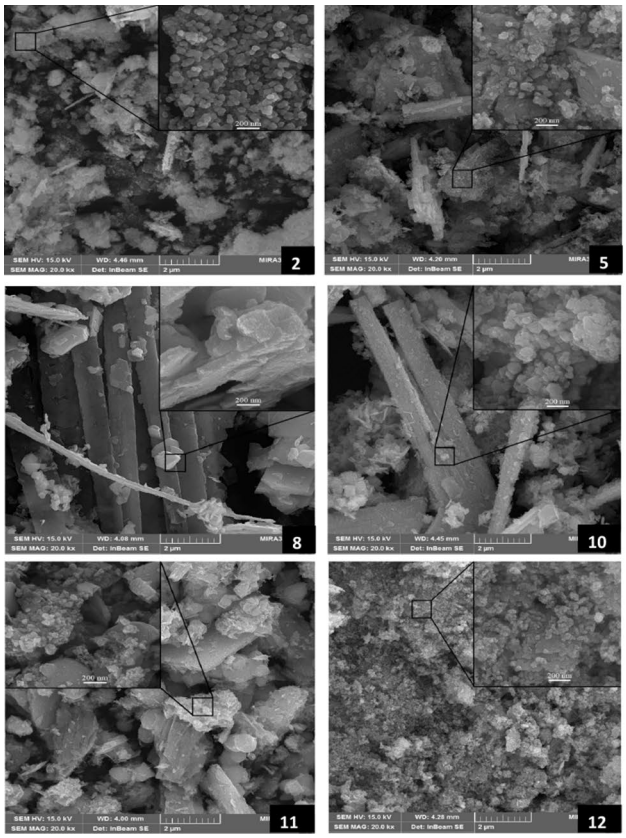


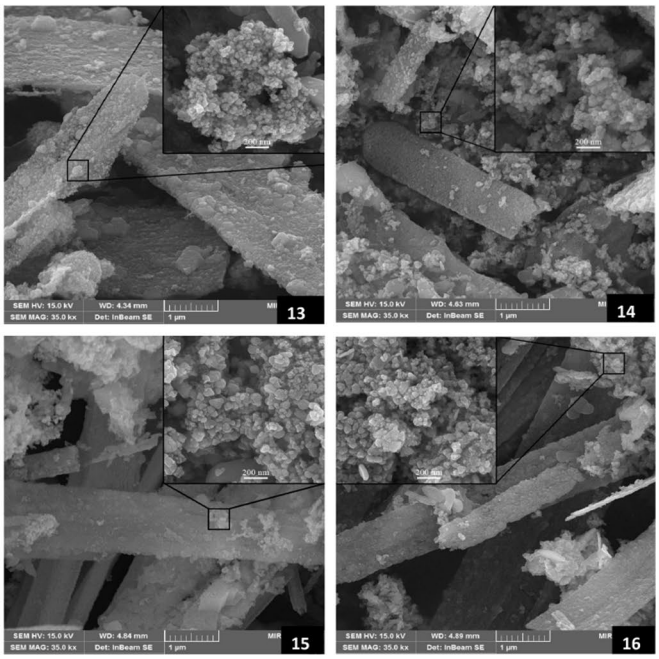


*Figure 8: The FESEM images of samples 2,5,8, 10-16*

**Fig. 8** FESEM images of samples 2, 5, 8, 10–16

## 7 Conclusion

For synthesis of CIGS Nps with solvothermal method, Cu, $In_{met}$, $InCl_3$, $GaCl_3$ and Se as precursors and ethylenediamine as solvent were used. Outcomes revealed that under $N_2$ atmosphere in autoclave, CGS and CIGS always are present together but in Ar atmosphere, if $In_{met}$ is used as In precursor, CGS and CIGS are formed together again, but by using $InCl_3$, $CuGaSe_2$ and $CuIn_{0.5}Ga_{0.5}Se_2$ single phases are produced. The optimum condition for synthesis of CGS and CIGS is annealing of the precursors at 185 and 175 °C for 12 h respectively, followed by extra annealing step at 230 °C for 24 h. These particles with size of about 20–25 nm and band gap of 1.78 and 1.39 eV for CGS and CIGS are proper for fabrication of CIGS solar cell.

**Acknowledgements** The authors are grateful to research council of the University of Kashan for providing financial support (Grant Number of 682128) to undertake this work.

## References

1. C.H. Lu, C.H. Lee, C.H. Wu, Sol. Energy Mater. Sol. Cells. **94**, 1622 (2010)
2. M. Wang, S.K. Batabyal, H.M. Lim, Z. Li, Y.M. Lam, J. Alloys Compd. **618**, 522 (2015)
3. S.H. Mousavi, T.S. Muller, P.W. de Oliveira, J. Colloid Interface Sci. **382**, 48 (2012)
4. B.P. Rand, J. Genoe, P. Heremans, J. Poortmans, Prog. Photovolt. Res. Appl. **15**, 659 (2015)
5. J.H. Woo, H. Yoon, J.H. Cha, D.Y. Jung, S.S. Yoon, J. Aerosol Sci. **54**, 1 (2012)
6. H. Lu, C. Yang, C. Lu, J. Mater. Sci. Mater. Electron. **27**, 10642 (2016)
7. Y. Lin, X. Peng, L. Wang, Y. Lin, C. Wu, S. Liang, J. Mater. Sci. Mater. Electron. **25**, 461 (2014)
8. M.E. Mohsen, B. Mostafa, J. Mater. Sci. Mater. Electron. (2015)
9. V.S. Saji, I.H. Choi, C.W. Lee, Sol. Energy. **85**, 2666 (2011)
10. B. Jeong, D.P. Norton, J.D. Budai, G.E. Jellison, Thin Solid Films. **446**, 18 (2004)
11. W. Wang, Y.W. Su, C.H. Chang, Sol. Energy Mater. Sol. Cells. **95**, 2616 (2011)
12. S. Ahn, K. Kim, K. Yoon, Curr. Appl. Phys. **8**, 766 (2008)
13. L. Fu, Y.Q. Guo, S. Zheng, Powder Diffr. **28**, S28 (2013)
14. W. Liu, D.B. Mitzi, M. Yuan, A.J. Kellock, S. Jay, O. Chey, Gunawan, Chem. Mater. **22**, 1010 (2010)
15. H. Lee, D. Jeong, T. Mun, B. Pejjai, V.R.M. Reddy, T.J. Anderson, C. Park, Korean J. Chem. Eng. **33**, 2486 (2016)
16. R.K. Wahi, Y. Liu, J.C. Falkner, V.L. Colvin, J. Colloid Interface Sci. **302**, 530 (2006)
17. S.I. Gu, S.H. Hong, H.S. Shin, Y.W. Hong, D.H. Yeo, J.H. Kim, S. Nahm, Ceram. Int. **38**, S521 (2012)

18. Y.G. Chun, K.H. Kim, K.H. Yoon, Thin Solid Films. **480–481**, 46 (2005)
19. S.H. Mousavi, T.S. Müller, R. Karos, P.W. De Oliveira, J. Alloys Compd. **659**, 178 (2016)
20. S. Hyo-Soon, G. Sin-Il, H. Seung-hyouk, H. Youn-Woo, Y. Dong-Hun, N. Sahn, J. Korean Phys. Soc. **57**, 1059 (2010)
21. M. Zahedifar, E. Ghanbari, M. Moradi, M. Saadat, Phys. Status Solidi Appl. Mater. Sci. **212**, 657 (2015)
22. F. Huang, A.H. Yan, H. Zhao, Z. Li, X.P. Cai, Y.H. Wang, Y.C. Wu, S.Bin Yin, Y.H. Qiang, Cryst. Res. Technol. **49**, 953 (2014)
23. A. Ben Marai, K. Djessas, Z. Ben, S. Ayadi, Alaya, J. Alloys Compd. **648**, 1038 (2015)
24. C.J. Hibberd, M. Ganchev, M. Kaelin, K. Ernits, A.N. Tiwari, in *2008 33rd IEEE Photovoltaic Specialists Conference (PVSC)*, p. 1 (2008)
25. F. Babbe, L. Choubrac, S. Siebentritt, F. Babbe, L. Choubrac, S. Siebentritt, 82105, 1142 (2016)
26. D. Abou-ras, S.S. Schmidt, N. Schäfer, J. Kavalakkatt, T. Rissom, T. Unold, R. Mainz, A. Weber, T. Kirchartz, E.S. Sanli, P.A. Van Aken, Q.M. Ramasse, H. Kleebe, D. Azulay, I. Balberg, O. Millo, O. Cojocaru-mirédin, D. Barragan-yani, K. Albe, J. Haarstrich, C. Ronning, Phys. Status Solidi Rapid Res. Lett. **375**, 363 (2016)
27. R. Noufi, R.J. Matson, R.C. Powell, C. Herrington, Sol. Cells. **16**, 479 (1986)
28. H. Neumann, R.D. Tomlinson, Sol. Cells. **28**, 301 (1990)
29. G. Voorwinden, R. Kniese, M. Powalla, Thin Solid Films. **431–432**, 538 (2003)
30. Y.C. Lin, W.T. Yen, Y.L. Chen, L.Q. Wang, F.W. Jih, Phys. B Condens. Matter. **406**, 824 (2011)
31. T. Feurer, P. Reinhard, E. Avancini, B. Bissig, J. Löckinger, P. Fuchs, R. Carron, T.P. Weiss, J. Perrenoud, S. Stutterheim, S. Buecheler, A.N. Tiwari, Prog. Photovoltaics Res. Appl. **25**, 645 (2017)
32. M. Sandberg, B. Moshfegh, Build. Environ. **37**, 211 (2002)
33. T. Zdanowicz, T. Rodziewicz, M. Zabkowska-Waclawek, Sol. Energy Mater. Sol. Cells. **87**, 757 (2005)
34. B. Li, Y. Xie, J. Huang, Y. Qian, Adv. Mater. **11**, 1456 (1999)
35. N.D. Abazović, D.J. Jovanović, M.M. Stoiljković, M.N. Mitrić, S.P. Ahrenkiel, J.M. Nedeljković, M.I. Čomor, J. Serbian Chem. Soc. **77**, 789 (2012)